HOKKAIDO UNIVERSITY

Title	Organic acids as efficient catalysts for group transfer polymerization of N,N-disubstituted acrylamide with silyl ketene acetal : polymerization mechanism and synthesis of diblock copolymers
Author(s)	Kikuchi, Seiya; Chen, Yougen; Kitano, Kodai; Takada, Kenji; Satoh, Toshifumi; Kakuchi, Toyoji
Citation	Polymer chemistry, 6(38), 6845-6856 https://doi.org/10.1039/c5py01104c
Issue Date	2015
Doc URL	http://hdl.handle.net/2115/62628
Type	article (author version)
File Information	Kakuchi-PC(6-38).pdf

Instructions for use

Hokkaido University Collection of Scholarly and Academic Papers : HUSCAP

Polymer Chemistry

RSCPublishing

ARTICLE

Organic Acids as Efficient Catalyst for Group Transfer Polymerization of *N,N*-Disubstituted Acrylamide with Silyl Ketene Acetal; Polymerization Mechanism and Synthesis of Diblock Copolymers

Cite this: DOI: 10.1039/x0xx00000x

Received 00th January 2012,
Accepted 00th January 2012

DOI: 10.1039/x0xx00000x

www.rsc.org/

Seiya Kikuchi,[a] Yougen Chen,[b] Kodai Kitano,[a] Kenji Takada,[c] Toshifumi Satoh,[c] and Toyoji Kakuchi [b, c]*

The group transfer polymerization (GTP) of *N,N*-diethylacrylamide (DEAA) was studied using various combinations of an organic acid of *N*-(trimethylsilyl)bis-(trifluoromethanesulfonyl)imide (Me_3SiNTf_2), 1-(2,3,4,5,6-pentafluorophenyl)-1,1-bis(trifluoromethanesulfonyl)methane ($C_6F_5CHTf_2$), and tris(pentafluorophenyl)borane ($B(C_6F_5)_3$) and a silyl ketene acetal (SKA) of 1-methoxy-1-(trimethylsiloxy)-2-methyl-1-propene (^{Me}SKA), 1-methoxy-1-(triethylsiloxy)-2-methyl-1-propene (^{Et}SKA), 1-methoxy-1-(triisopropylsiloxy)-2-methyl-1-propene (^{iPr}SKA), and 1-methoxy-1-(triphenylsiloxy)-2-methyl-1-propene (^{Ph}SKA), among which the combination of $B(C_6F_5)_3$ and ^{Et}SKA afforded a relatively better control over the molecular weight distribution. The polymerization behavior of DEAA using $B(C_6F_5)_3$ and ^{Et}SKA was then intensively investigated in terms of the polymerization kinetics, chain extension experiments, and MALDI-TOF MS analyses, by which the polymerization was proven to proceed in a living fashion though an induction period of tens of minutes occurred. The $B(C_6F_5)_3$-catalyzed GTP was further extended to various *N,N*-disubstituted acrylamides (DAAs), such as *N,N*-dimethylacrylamide (DMAA), *N,N*-di-*n*-propylacrylamide (D*n*PAA), *N*-acryloylpiperidine (API), *N*-acryloylmorpholine (NAM), *N*-(2-methoxyethyl)-*N*-methylacrylamide (MMEAA), *N,N*-bis(2-methoxyethyl)acrylamide (BMEAA), *N,N*-diallylacrylamide (DVAA), and *N*-methyl-*N*-propargylacrylamide (MPAA). Finally, the livingness of the polymerization was used to synthesize acrylamide-acrylamide block copolymers and methacrylate-acrylamide hetero block copolymers.

Introduction

Polyacrylamides are a sort of important polymer materials for industrial applications, such as flocculants,[1] viscosifiers for oil recovery, and subdermal fillers for aesthetic facial surgery. [2] Although most of the industrial polyacrylamide products have been undoubtedly prepared by conventional radical polymerizations, the precise, efficient, and green synthesis of such polyacrylamides is still an interesting subject from the viewpoint of polymer synthesis. The living polymerization of various acrylamides has been achieved by the living/controlled radical polymerizations (CRPs), such as atom transfer radical polymerization,[3,4] nitroxide-mediated radical transfer polymerization, [6-8] and anionic polymerization. These CRPs are applicable to acrylamide, *N*-monosubstituted acrylamide, and *N,N*-disubstituted acrylamide (DAA) except for those bearing radical-sensitive groups, such as *N*-allyl acrylamide and *N*-2-thioethyl acrylamide. On the other hand, anionic polymerization is only suitable for DAAs without any anion-sensitive groups though applicable DAAs are limited to *N,N*-dimethylacrylamide (DMAA),[9-11] *N,N*-diethylacrylamide (DEAA),[10-13] *N,N*-di-*n*-propylacrylamide (D*n*PAA),[11] *N*-ethylmethylacrylamide (EMA),[11] *N*-acryloylpyrrolidine (APY),[11] *N*-acryloylpiperidine (API),[11] *N*-acryloylmorpholine (NAM),[11] *N*-acryloyl-2-methylaziridine,[14] *N*-acryloylazetidine,[15] *N*-methoxymethyl-*N*-isopropylacrylamide,[16] *N*-propyl-*N*-(3-triisopropoxysilylpropyl)acrylamide,[17] and *N*-propyl-*N*-(3-triethoxysilylpropyl)acrylamide.[17] Nevertheless, the anionic polymerization of DAA is still the most reliable method for the precise synthesis of the structurally defect-free polyacrylamides because the CRPs inevitably cause side reactions due to radical transfers.

Scheme 1. Syntheses of homo acrylamide polymers, homo acrylamide block copolymers, and hetero block copolymers by organic acid-catalyzed group transfer polymerization method.

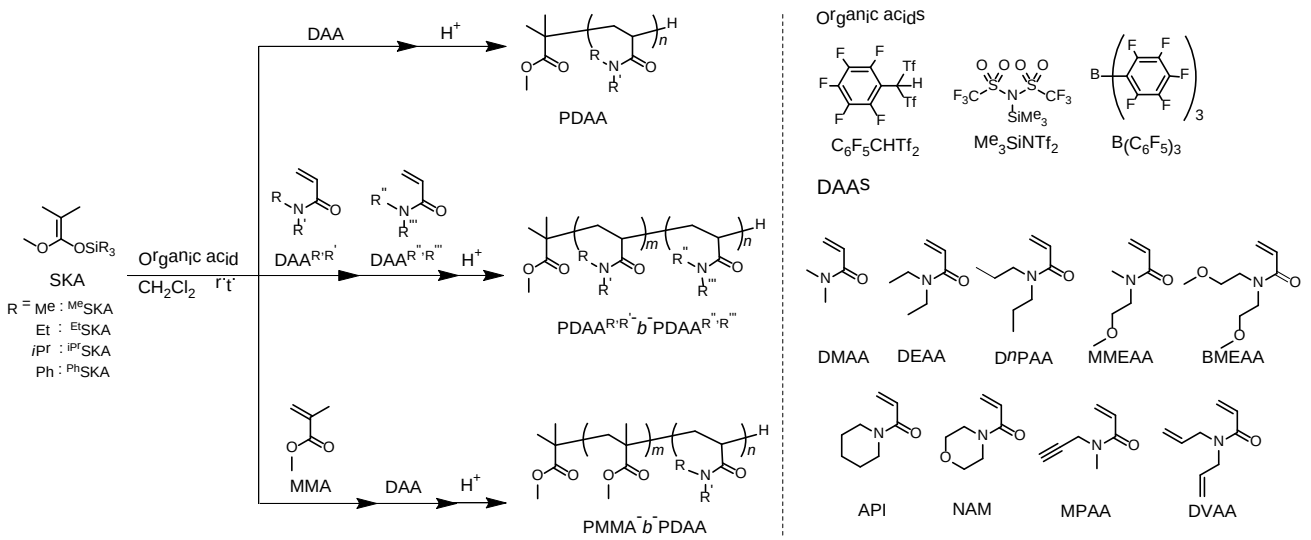

Hence, we turned our attention to the group transfer polymerization (GTP), one of the anionic polymerization methods, which is principally suitable for acrylic monomers.[18-21] The living polymer chain-ends capped by silyl groups in the GTP process are much less reactive than the living anions during the anionic polymerization processes, which is one of the reasons why the GTP proceeds at a moderate temperature and is tolerant to functional moieties, such as vinyl and epoxy groups.[22, 23] In particular, the use of organocatalysts for the GTP of methacrylate and acrylate monomers has significantly improved the livingness of the polymerizations leading to well defined polymers with high molecular weights. [24-34] In addition, organocatalysts significantly improved the controlled/living characteristics for the GTP of acrylamides compared to previous methods those using conventional catalysts; [18,19,35-37] for example, we reported that organic Brønsted acids, such as bis(trifluoromethanesulfonyl)imide ($HNTf_2$) and 1-(2,3,4,5,6-pentafluorophenyl)-1,1-bis(trifluoromethanesulfonyl)methane ($C_6F_5CHTf_2$), were used for the controlled GTP of DMAA with a silyl ketene aminal of (*Z*)-1-dimethylamino-1-trimethylsiloxy-1-propene ((*Z*)-DATP) as the initiator to produce poly(*N*,*N*-dimethylacrylamide)s with molecular weights up to 53.9 kg mol^{-1} and polydispersities of less than 1.06, which was the first report to achieve the living polymerization of DAA in the GTP chemistry.[38,39] Furthermore, Taton and Gnanou reported that *N*-heterocyclic carbene was used as an efficient organocatalyst for the GTP of DMAA and the block GTP of DMAA and methyl methacrylate to produce tailored polyacrylamides and diblock copolymers.[40,41] Thus, of great importance is to elucidate the scope and limit for the GTP of DAA in terms of applicable monomers, available organocatalysts, and initiator design. For example, it is interesting to expand the applicable monomers, such as the DAAs with nucleophilic hetero atoms of oxygen, nitrogen, and sulfur, because these atoms would deactivate the true catalytic species of a silylium cation. In addition, the $HNTf_2$-catalyzed GTP of DMAA required the use of the silyl ketene aminal though its synthesis turned out to be more difficult than a silyl ketene acetal (SKA), and the GTP with the silyl ketene aminal as the initiator could not be used to synthesize hetero block copolymers because the silyl ketene aminal group of the growing polymer chain-end could not initiate the GTP of the methacrylate and acrylate monomers. Thus, the comprehensive study for the GTP of DAA coupled with available organocatalysts and initiator design is still one of the challenging and remaining tasks in GTP chemistry.

We now report the new efficient combinations of organic acids and SKAs for the GTPs of various DAAs, as shown in Scheme 1. This study describes: (1) the evaluation of the combinations of organic acids and SKAs for the GTP of DEAA, (2) the investigation of the livingness and mechanism of the $B(C_6F_5)_3$-catalyzed GTP of DAAs, (3) the monomer expansion, and (4) the synthesis of homo and hetero block copolymers.

Experimental Section

Materials. Dichloromethane (CH_2Cl_2, >99.5%; water content, <0.001%), methanol (MeOH), and deuterated chloroform

($CDCl_3$, > 99.8%) were purchased from Kanto Chemicals Co., Inc. *N*,*N*-Diethylacrylamide (DEAA), 1-methoxy-1-trimethylsiloxy-2-methyl-1-propene (^{Me}SKA), *N*-(trimethylsilyl)bis(trifluoromethanesulfonyl)imide (Me_3SiNTf_2), 1-(2,3,4,5,6-pentafluorophenyl)-1,1-bis(trifluoromethane-sulfonyl)methane ($C_6F_5CHTf_2$), *trans*-3-indoleacrylic acid, *N*,*N*-dimethyl acrylamide (DMAA), *N*-acryloylmorpholine (NAM), and methyl methacrylate (MMA) were purchased from Tokyo Kasei Kogyo Co., Ltd. 1-*tert*-Butyl-4,4,4-tris(dimethylamino)-2,2-bis[tris(dimethylamino)-phosphoranylidenamino]-2Λ^5,4Λ^5-catenadi(phosphazene) (*t*-Bu-P_4, 1.0 mol L^{-1} in *n*-hexane) and sodium trifluoroacetate were purchased from the Sigma-Aldrich Chemicals Co. Tris(pentafluorophenyl)borane ($B(C_6F_5)_3$) was purchased from Wako Pure Chemical Industries, Ltd., and was used after recrystallization from *n*-hexane at −30 °C. DEAA, DMAA, NAM, MMA, and CH_2Cl_2 were distilled from CaH_2, degassed by three freeze-pump-thaw cycles, and stored under an Ar atmosphere prior to use. 1-Methoxy-1-(triethylsiloxy)-2-methyl-1-propene (^{Et}SKA),[42] 1-methoxy-1-(triisopropyl siloxy)-2-methyl-1-propene (^{iPr}SKA), and 1-methoxy-1-(triphenylsiloxy)-2-methyl-1-propene (^{Ph}SKA) were synthesized according to previous reports.[43] The Spectra/Por® 6 Membrane (MWCO: 1000) was used for the dialysis. All other chemicals were purchased from available suppliers and used without purification.

Measurements. The ^{1}H (400 MHz) and ^{13}C NMR (100 MHz) spectra were recorded using a JEOL ECS400. The preparation of the polymerization solution was carried out in an MBRAUN stainless steel glove box equipped with a gas purification system (molecular sieves and copper catalyst) and a dry argon atmosphere (H_2O, O_2 <1 ppm). The moisture and oxygen contents in the glove box were monitored by an MB-MO-SE 1 and MB-OX-SE 1, respectively. Size exclusion chromatography (SEC) in DMF containing lithium chloride (0.01 mol L^{-1}) was performed at 40 °C using a Jasco high performance liquid chromatography (HPLC) system (PU-980 Intelligent HPLC pump, CO-965 column oven, RI-930 Intelligent RI detector, and Shodex DEGAS KT-16) equipped with a Shodex Asahipak GF-310 HQ column (linear, 7.6 mm × 300 mm; pore size, 20 nm; bead size, 5 μm; exclusion limit, 4×10^4) and a Shodex Asahipak GF-7M HQ column (linear, 7.6 mm × 300 mm; pore size, 20 nm; bead size, 9 μm; exclusion limit, 4×10^7) at the flow rate of 0.6 mL min^{-1}. The $M_{n,SEC}$ and M_w/M_n of the obtained polymers were determined by the RI based on poly(methyl methacrylate) (PMMA) with the M_w (M_w/M_n)s of 1.25×10^6 g mol^{-1} (1.07), 6.59×10^5 g mol^{-1} (1.02), 3.003×10^5 g mol^{-1} (1.02), 1.385×10^5 g mol^{-1} (1.05), 6.015×10^4 g mol^{-1} (1.03), 3.053×10^4 g mol^{-1} (1.02), and 1.155×10^4 g mol^{-1} (1.04), 4.90×10^3 g mol^{-1} (1.10), 2.87×10^3 g mol^{-1} (1.06), and 1.43×10^3 g mol^{-1} (1.15), respectively. The matrix-assisted laser desorption/ionization time-of-flight mass spectrometry (MALDI-TOF MS) measurements were performed using an Applied Biosystems Voyager-DE STR-H mass spectrometer with a 25 kV acceleration voltage. The positive ions were detected in the reflector mode (25 kV). A nitrogen laser (337 nm, 3 ns pulse width, 106–107 W cm^{-2}) operating at 3 Hz was used to produce the laser desorption, and the 200 shots were summed. The spectra were externally calibrated using a sample prepared from narrow-dispersed polystyrene (Chemco Scientific Co., Ltd., M_n = 3.6 kg mol^{-1}, M_w/M_n = 1.08, 30 μL, 10 mg mL^{-1} in THF), the matrix (1,8-dihydroxy-9-(10*H*)-anthracenone, 30 mg mL^{-1}, 100 μL), and the cationizing agent (silver trifluoroacetate, 10 mg mL^{-1}, 15 μL) with a linear calibration. Samples for the MALDI-TOF MS were prepared by mixing the polymer (1.5 mg mL^{-1}, 10 μL), the matrix (*trans*-3-indoleacrylic acid, 10 mg mL^{-1}, 90 μL), and the cationizing agent (sodium trifluoroacetate, 10 mg mL^{-1}, 10 μL) in THF.

Polymerization of acrylamide monomers. A typical procedure for the polymerization is as follows. A stock solution (40.0 μL, 2.00 μmol) of $B(C_6F_5)_3$ in CH_2Cl_2 (0.05 mol L^{-1}) was added to a solution of DEAA (127 mg, 1.00 mmol) and ^{Et}SKA (8.65 mg, 40.0 μmol) in CH_2Cl_2 (1.81 mL) at room temperature (25 °C). After 70 min of the polymerization, MeOH was added to the solution to quench the polymerization. The crude product was purified by dialysis against MeOH followed by lyophilization of the resulting polymers from their aqueous solutions. Yield: 80.0 mg (63%); SEC (RI): $M_{n,SEC}$ = 3.36 kg mol^{-1}, M_w/M_n = 1.14. In the post polymerization experiments and block copolymerizations, the additional monomer was added to the reaction mixture just after a small portion of the reaction mixture was taken for the determination of the monomer conversion and the $M_{n,SEC}$ and M_w/M_n of the product in the first polymerization.

Results and discussion

GTP of *N*,*N*-diethylacrylamide using various organic acids and silyl ketene acetals. The GTP of *N*,*N*-diethylacrylamide (DEAA) was carried out using various organocatalysts and silyl ketene acetals (SKAs), such as ^{Me}SKA, ^{Et}SKA, ^{iPr}SKA, and ^{Ph}SKA, in CH_2Cl_2 at room temperature (~25 °C) to find a suitable combination of a catalyst and an initiator for the controlled/living GTP of DEAA. We employed three types of organocatalysts, such as the Lewis acid of tris(pentafluorophenyl)borane ($B(C_6F_5)_3$) and *N*-(trimethylsilyl)triflylimide (Me_3SiNTf_2), the Brønsted acid of pentafluorophenylbis(triflyl)methane ($C_6F_5CHTf_2$), and the Lewis base of *t*-Bu-P_4, which have been previously reported as efficient catalysts for the GTP of (meth)acrylates.[24] The polymerizations of DEAA were carried out under the conditions of $[DEAA]_0$ = 0.5 mol L^{-1} and $[DEAA]_0/[Initiator]_0$ = 50, and the polymerization results are summarized in Table 1. The acidic organic catalysts were obviously more effective than the basic catalyst of *t*-Bu-P_4, since the molecular weights obtained from the acid-catalyzed GTP were better controlled. Given that the *t*-Bu-P_4-catalyzed GTP proceeding through the dissociative mechanism, in which the active species was an enolate anion conjugating with a carbanion, was rather similar to the conventional anionic polymerization, the propagating ends of the enolate anions were so reactive that they readily caused side reactions or termination reactions which led to broad molecular weight distributions (MWDs) or no polymerization. We reported that the GTPs of acrylates, such as methyl acrylate and *n*-butyl acrylate, using the acidic catalysts

smoothly proceeded in a quantitative monomer conversion by optimizing the bulkiness of the silyl group of the employed SKA, in which $^{i\text{Pr}}$SKA was found to be the most effective initiator for preparing the corresponding well-defined polymers.[34] In this study, all the acid-catalyzed GTPs of DEAA were completed with quantitative monomer consumption within the set polymerization times except for the $B(C_6F_5)_3$-catalyzed polymerization using $^{i\text{Pr}}$SKA. The acid-catalyzed polymerizations using $^{\text{Me}}$SKA and $^{\text{Ph}}$SKA (runs 5, 8, 9, 12, 13 and 16) afforded broad MWDs as M_w/M_ns >1.22 and those using $^{i\text{Pr}}$SKA (runs 7 and 11) produced poly(*N*,*N*-diethylacrylamide)s (PDEAAs) with MWDs of 1.19. In contrast, the polymerizations using $^{\text{Et}}$SKA with a moderately bulky silyl group produced the most narrowly-distributed PDEAAs, among which the $B(C_6F_5)_3$-catalyzed polymerization afforded the narrowest MWD. The number-averaged molecular weights ($M_{n,SEC}$s) of these resulting PDEAAs were estimated using size exclusion chromatography based on PMMA standards due to the lack of appropriate PDEAA standards, meaning that the $M_{n,SEC}$ values should be slightly deviated from the exact values. In this study, we mainly used the MWD as the evaluating criterion and thus selected $B(C_6F_5)_3$ as the catalyst for the following polymerizations due to its operating convenience, unless otherwise instructed.

Living nature of the $B(C_6F_5)_3$-catalyzed GTP of DEAA. The living nature of the $B(C_6F_5)_3$-catalyzed GTP of DEAA was assessed by the kinetic studies, the MALDI-TOF MS measurements, and the post-polymerization experiments. The polymerization using $^{\text{Et}}$SKA for the kinetic study was implemented in CH_2Cl_2 at 25 °C, $[DEAA]_0/[^{\text{Et}}SKA]_0/[B(C_6F_5)_3]_0$ = 25/1/0.05, and $[DEAA]_0$ = 0.5 mol L^{-1}. Figure 1 shows the zero- and first-order kinetic plots and the $M_{n,SEC}$ and M_w/M_n dependence on the monomer conversion (Conv.). Surprisingly, the kinetic plots displayed a distinct induction period of ca. 25 min, which is likely to suggest that the propagation reaction was much faster than the initiation reaction. The further discussion in this regard is described in greater detail in the following section about polymerization mechanism. After the induction period, the polymerization normally proceeded as a propagation reaction till the complete consumption of the monomer in 20 min, during which no retardation of the polymerization was observed, indicating that no termination reaction occurred during the entire propagation process. The polymerization turned out to be zero-order, rather than a first-order reaction. The $M_{n,SEC}$ and M_w/M_n dependence on the monomer conversion (Conv.) shown in Figure 1(b) indicated that the $M_{n,SEC}$ of the obtained PDEAA linearly increased from 1.65 to 4.00 kg mol^{-1} with the increasing monomer conversion, while their M_w/M_ns were as narrow as <1.17, which indicated the homogeneous growth of the PDEAA chain in the propagation stage. Excluding the induction period, the above polymerization possessed true living characteristics.

Table 1. Organocatalyzed GTPs of DEAA using various SKAs at room temperature (~ 25 °C)

run	Catalyst (Cat.)	Initiator (I)	$[DEAA]_0/[I]_0/[Cat.]_0$	Time (h)	Conv. (%) [b]	$M_{n,SEC}$ [c] ($M_{n,calcd.}$ [d]) (kg mol^{-1})	M_w/M_n [c]
1	*t*-Bu-P_4 [e]	$^{\text{Me}}$SKA	50/1/0.05	24	55.5	3.74 (3.53)	2.4 [f]
2		$^{\text{Et}}$SKA		24	32.2	5.96 (2.15)	12.4 [f]
3		$^{i\text{Pr}}$SKA		24	<1	n.d. [g]	n.d. [g]
4		$^{\text{Ph}}$SKA		24	<1	n.d. [g]	n.d. [g]
5	Me_3SiNTf_2	$^{\text{Me}}$SKA	50/1/0.02	2	>99	6.95 (6.45)	1.24
6		$^{\text{Et}}$SKA		2	>99	5.60 (6.45)	1.22
7		$^{i\text{Pr}}$SKA		24	>99	4.09 (6.45)	1.19
8		$^{\text{Ph}}$SKA		2	>99	7.04 (6.45)	1.28
9	$C_6F_5CHTf_2$	$^{\text{Me}}$SKA	50/1/0.02	2	>99	6.40 (6.45)	1.22
10		$^{\text{Et}}$SKA		2	>99	5.90 (6.45)	1.18
11		$^{i\text{Pr}}$SKA		23	>99	3.82 (6.45)	1.19
12		$^{\text{Ph}}$SKA		2	>99	5.84 (6.45)	1.27
13	$B(C_6F_5)_3$	$^{\text{Me}}$SKA	50/1/0.05	2.5	>99	6.68 (6.45)	1.23
14		$^{\text{Et}}$SKA		3.0	>99	5.18 (6.45)	1.16
15		$^{i\text{Pr}}$SKA		20	<1	n.d. [g]	n.d. [g]
16		$^{\text{Ph}}$SKA		20	>99	6.73 (6.45)	1.26

[a] Ar atmosphere; $[DEAA]_0$ = 0.5 mol L^{-1}; solvent, CH_2Cl_2. [b] Determined by ^{1}H NMR in $CDCl_3$. [c] Determined by SEC in DMF containing 0.01 mol L^{-1} LiCl calibrated with PMMA. [d] Calculated from $[DEAA]_0/[I]_0$ × (MW of DEAA = 127.18) × Conv. + (MW of initiator residue = 102.13). [e] Solvent, toluene. [f] Shape of SEC trace was bimodal. [g] Not determined.

This journal is © The Royal Society of Chemistry 2012

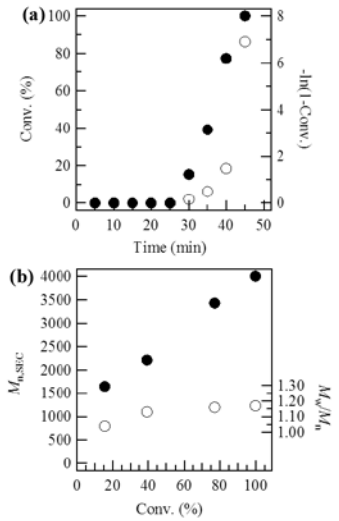

Figure 1. (a) Zero- (●) and first- (○) order kinetic plots of the $B(C_6F_5)_3$-catalyzed GTP of DEAA at 25 °C under the conditions of $[DEAA]_0/[^{Et}SKA]_0/[B(C_6F_5)_3]_0$ = 25/1/0.05 and $[DEAA]_0$ = 0.50 mol L^{-1} and (b) Dependence of $M_{n,SEC}$ (●) and M_w/M_n (○) of the obtained PDEAA on monomer conversion (Conv.).

A MALDI-TOF MS spectrum of the obtained PDEAA in Figure 2 provided a more detailed insight into the chemical structure of the resulting polymer and further into the polymerization reaction. The spectrum showed only one population of molecular ion peaks and the distance between any two neighboring molecular ion peaks was ca. 126.9 Da, which well corresponded to the exact molecular weight of DEAA as the repeating unit. In addition, the *m*/*z* value of each molecular ion peak definitely suggested the sodium-cationized polymer composition of [MeO_2CMe_2C-$DEAA_n$-H + Na^+] (molecular formula: $C_{7n+5}H_{13n+10}N_nO_{n+2}Na$), *e.g.*, the *m*/*z* value of 3302.33 Da for a specified peak corresponded to a sodium-cationized 25-mer polymer structure of [MeO_2CMe_2C-$DEAA_{25}$-H + Na^+] with the theoretical monoisotopic value of 3302.55 (molecular formula: $C_{180}H_{335}O_{27}N_{25}Na$). This result strongly supported the fact that the polymerization proceeded without any side-reactions. However, the molecular ion peaks had a broad distribution ranging from 1500 to 9000 Da, which is considered to be caused by the lower initiation rate than that of the propagation. The initiating end was also confirmed by the ^1H NMR measurements, *i.e.*, the methoxy protons of the ^{Et}SKA residue at the α-terminal of PDEAA was clearly observed at 3.64 ppm (peak b) along with those due to the main-chain protons of PDEAA at 0.82-1.98 (peaks c and f), 2.20-2.86 (peak d), and 2.90-3.62 (peak e) ppm (Figure S2(a)).

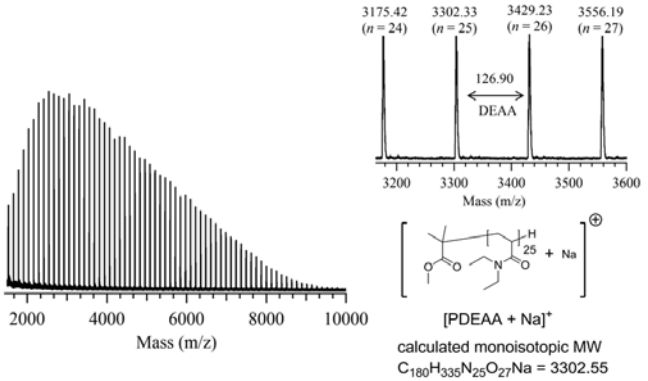

Figure 2. MALDI-TOF MS spectrum of a low molecular weight PDEAA ($M_{n,SEC}$ = 3.36 kg mol^{-1}, M_w/M_n = 1.14) obtained from the GTP of DEAA using ^{Et}SKA.

The chain extension experiment was further carried out to prove the living nature of the propagating end of PDEAA. Under the conditions of $[DEAA]_0/[^{Et}SKA]_0/[B(C_6F_5)_3]_0$ = 25/1/0.05 in CH_2Cl_2 at room temperature (~25°C), 25 equivalents of DEAA were initially polymerized for 80 min to afford a quantitative monomer conversion and an intermediate PDEAA product with $M_{n,SEC}$ of 3.20 kg mol^{-1} and M_w/M_n of 1.18. After the polymerization mixture was placed in the argon atmosphere for a short time, another fresh 50 equivalents of DEAA were further added to the polymerization system to observe the chain extension behavior. The second-stage polymerization was completed within 80 min with a quantitative monomer conversion to afford the final PDEAA product with the $M_{n,SEC}$ of 7.33 kg mol^{-1} and the M_w/M_n of 1.22. The SEC traces of the first- and second-stage PDEAAs are shown in Figure 3(a), in which the SEC trace obtained from the second-stage polymerization exhibited a rather clear shift toward the high molecular weight region when referred to the one obtained from the first-stage polymerization. This result definitely indicated that the propagating end of the growing PDEAA possessed a truly living propagation end, which brought about the chain extension after the sequential addition of the monomer. In summary, the living nature of the $B(C_6F_5)_3$-catalyzed GTP of DEAA using ^{Et}SKA was proved by all of the above results.

The living characteristics of this polymerization system were used to prepare various PDEAAs with different molecular weights by varying the $[DEAA]_0/[^{Et}SKA]_0$ ratios from 25 to 200 under a fixed $[B(C_6F_5)_3]_0/[^{Et}SKA]_0$ ratio of 0.05. All the polymerizations underwent a quantitative monomer consumption and the SEC traces of the obtained polymers in Figure 3(b) showed mono-distributions, from which the $M_{n,SEC}$ (kg mol^{-1}) (M_w/M_n)s were estimated to be 3.36 (1.14), 5.18 (1.16), 10.3 (1.21), and 21.5 (1.24),

corresponding to the related $[DEAA]_0/[^{Et}SKA]_0$ ratios of 25, 50, 100, and 200, respectively.

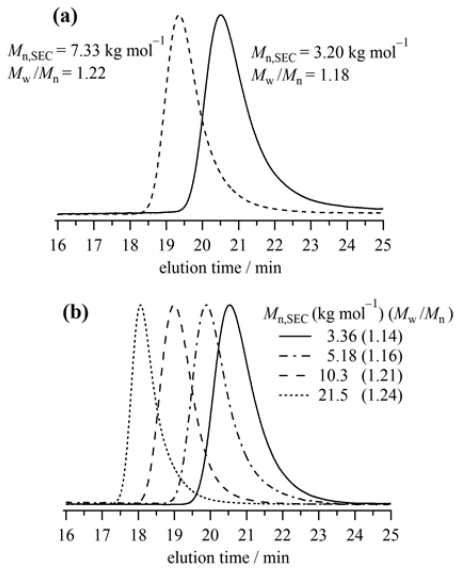

Figure 3. SEC traces of the PDEAA products obtained from (a) the first-stage PDEAA (solid line) and the second-stage PDEAA (dashed line) in the chain extension experiment and (b) various $[DEAA]_0/[^{Et}SKA]_0$ ratios of 25, 50, 100, and 200.

Mechanism of the $B(C_6F_5)_3$-catalyzed GTP of DEAA. Given the unique polymerization behavior of the $B(C_6F_5)_3$-catalyzed GTP of DEAA using ^{Et}SKA, we proposed a plausible mechanism, as shown in Scheme 2. The $B(C_6F_5)_3$-catalyzed GTP of DEAA has three elementary reactions, including (1) monomer activation by $B(C_6F_5)_3$, (2) initiation reaction, and (3) propagation reaction. For (1), it was reported that an aromatic amide showed an extremely high coordination affinity toward the highly electrophilic $B(C_6F_5)_3$ and the equilibria lay far toward the formation of coordination adducts (a high equilibrium constant).[44] This trend is also adaptable to the α-unsaturated amide of DEAA in our case. As shown in Figure 4(a), the proton signals of the equimolar mixture of DEAA and $B(C_6F_5)_3$ for $[DEAA]_0 = [B(C_6F_5)_3]_0 = 0.167$ mol L^{-1} showed very clear chemical shifts, which suggests the formation of the coordinating products of DEAA*. In addition, each peak showed an almost complete shift, indicating the equilibrium constant (K_{eq}) for (1) is rather high though we did not calculate the exact K_{eq} value. The high K_{eq} implies that $B(C_6F_5)_3$ in the solution mixture almost exists in the DEAA*. It should be noted that the signals due to the vinyl protons of DEAA showed an upfield shift after coordinating with $B(C_6F_5)_3$, while those due to the ethyl group showed a downfield shift. This result might indicate that $B(C_6F_5)_3$ is located in an *anti* fashion toward the diethylamino group of DEAA because the upfield shift is considered to be caused by the ring current effect of the pentafluorophenyl ring of $B(C_6F_5)_3$. The monomer activation was also verified by ^{13}C NMR measurements, as shown in Figure 4(b). For (2), the initiation reaction occurs between the ^{Et}SKA and DEAA* and produces a silyl ketene aminal from the silyl ketene acetal of ^{Et}SKA. The initiation reaction turns out to slowly proceed and shows a distinct induction period. This phenomenon can be firmly attributed to the mismatch of the chemical structures between ^{Et}SKA and DEAA because the $B(C_6F_5)_3$-catalyzed GTP of DEAA using a silyl ketene aminal does not have such an induction period, as determined in our unpublished study. When comparing the structures of ^{Et}SKA and the generated silyl ketene aminal, the ^{Et}SKA has an additional methyl group bonded to the ene group, which hinders the initiation reaction; on the other hand, the acetal group in ^{Et}SKA has a lower electron-donating ability than that of the aminal group in the silyl ketene aminal, which indicates that the ene group of ^{Et}SKA is less nucleophilic toward DEAA* in comparison to that of the silyl ketene aminal. Therefore, these two structural factors of ^{Et}SKA result in the induction period and relatively slow initiation reaction. This fact, in turn, suggests that it is of great significance to design the initiator possessing a similar structure with the monomer. For (3), the propagation reaction shows the living characteristics commonly appearing in a living polymerization. It should be emphasized that the propagation reaction of this polymerization system is strongly suggested to be a zero-order reaction, as shown in Figure 1(a). This can be well explained by the following description. As a premise, the propagation rate (k_p) in each addition reaction is assumed to be a constant. The total monomer consumption rate can then be expressed as

$$-\frac{d[DEAA]}{dt} = k_p[SKA][DEAA^*] \qquad \text{(i)}$$

It is assumed that no side reactions take place during the polymerization process. Thus,

$$[SKA] = [^{Et}SKA]_0 \qquad \text{(ii)}$$

Considering that the real-time [DEAA] is much higher than $[B(C_6F_5)_3]$ and K_{eq} is significantly high, it is thus rational to assume that the [DEAA*] remains constant, the same as $[B(C_6F_5)_3]_0$, except for the very late time of the entire propagation period. Thus,

$$[DEAA^*] = [B(C_6F_5)_3]_0 \qquad \text{(iii)}$$

Equation (iv) is derived from equations (i), (ii), and (iii) as

$$[DEAA]_0 - [DEAA] = k_p\left[^{Et}SKA\right]_0[B(C_6F_5)_3]_0 t \qquad \text{(iv)}$$

Namely,

$$\text{Conv.}(\%) = \frac{k_p\left[^{Et}SKA\right]_0[B(C_6F_5)_3]_0 t}{[DEAA]_0} \times 100\% \qquad \text{(v)}$$

in which k_p, $[^{Et}SKA]_0$, $[DEAA]_0$, and $[B(C_6F_5)_3]_0$ are constants and t is the given polymerization time. We define the observed rate constant as $k_{p.obs.} = \frac{k_p\left[^{Et}SKA\right]_0[B(C_6F_5)_3]_0}{[DEAA]_0}$s. Thus, equation (v) can be changed to

$$\text{Conv.}(\%) = k_{p.obs.} t \times 100\% \qquad \text{(vi)}$$

When the induction time (t_i) is taken into consideration, the corrected equations, (vii) and (viii), can be obtained as

$$\text{Conv.}(\%) = 0 \qquad (t \le t_i) \qquad \text{(vii)}$$

This journal is © The Royal Society of Chemistry 2012

$$\text{Conv.}(\%) = k_{p.obs.}(t - t_i) \times 100\% \quad (t > t_i) \qquad \text{(viii)}$$

Obviously, the propagation is a zero-order reaction. During the propagation period, the monomer consumption is linearly dependent on the polymerization time once the initial conditions are fixed, except for that in the late stage of the propagation period due to the changing [DEAA*] after consumption of most of the monomer, and independent of the monomer concentration, which has also been fully reflected in the following zero-order kinetic plots of the $B(C_6F_5)_3$-catalyzed GTPs of other acrylamide monomers (Figure 5).

Scheme 2. A plausible mechanism for the $B(C_6F_5)_3$-catalyzed GTP

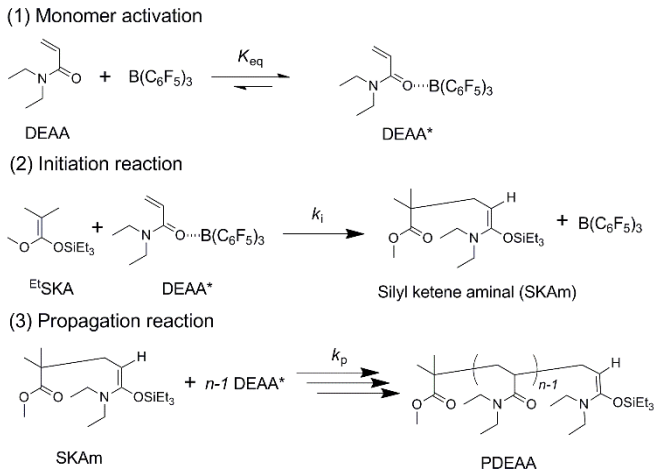

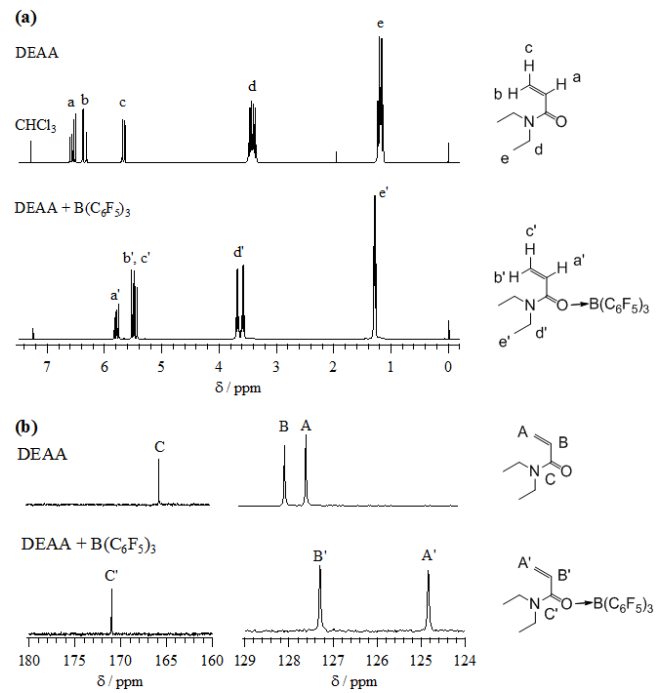

Figure 4. (a) ^{1}H and (b) ^{13}C NMR spectra of DEAA and an equimolar mixture of DEAA and $B(C_6F_5)_3$ ($[DEAA]_0$ = $[B(C_6F_5)_3]_0$ = 0.167 mol L^{-1}) in $CDCl_3$.

$B(C_6F_5)_3$-catalyzed GTPs of various *N*,*N*-disubstituted acrylamides. To explore the suitability of this polymerization, we further applied this method to various *N*,*N*-disubstituted acrylamide monomers (Scheme 1), such as *N*,*N*-dimethylacrylamide (DMAA), *N*,*N*-di-*n*-propylacrylamide (D*n*PAA), *N*-acryloylpiperidine (API), *N*-acryloylmorpholine (NAM), *N*-(2-methoxyethyl)-*N*-methylacrylamide (MMEAA), *N*,*N*-bis(2-methoxyethyl)acrylamide (BMEAA), *N*,*N*-diallylacrylamide (DVAA), and *N*-methyl-*N*-propargylacrylamide (MPAA), to synthesize their corresponding acrylamide polymers, among which poly(*N*,*N*-dimethylacrylamide) (PDMAA) and poly(*N*-acryloylmolpholine) (PNAM) are water-soluble; poly(*N*,*N*-di-*n*-propylacrylamide) (PD*n*PAA) and poly(*N*-acryloylpiperidine) (PAPI) are water-insoluble; poly(*N*-acryloylmolpholine) (PNAM), poly(*N*-(2-methoxyethyl)-*N*-methylacrylamide) (PMMEAA), and poly(*N*,*N*-bis(2-methoxyethyl)acrylamide) (PBMEAA) are thermoresponsive; poly(*N*,*N*-diallylacrylamide) (PDVAA) and poly(*N*-methyl-*N*-propargylacrylamide) (PMPAA) are functionalized and reactive. The polymerizations were done in CH_2Cl_2 at room temperature by optimizing the parameters in terms of the $[monomer]_0/[^{Et}SKA]_0$ ratio, monomer concentration, the polymerization time, and the catalyst amount, depensing on the monomer used; their polymerization results are summarized in Table 2. All the polymerizations homogeneously proceeded and gave quantitative monomer conversions within the set polymerization time. The $M_{n,SEC}$s estimated by the SEC measurements (Figure S1) of the obtained PDMAA, PD*n*PAA, PAPI, PNAM, PMMEAA, PBMEAA, PDVAA, and PMPAA were 6.35, 14.7, 8.65, 13.5, 8.40, 16.2, 13.5, 8.44 kg mol^{-1} when their corresponding $[monomer]_0/[^{Et}SKA]_0$ ratios were 100, 100, 100, 100, 50, 100, 100, 50, respectively. It should be emphasized that it is meaningless to do the comparison between the $M_{n,SEC}$s and the theoretical molecular weights ($M_{n,calcd.}$s) because of the inconsistency between the obtained polymers and the PMMA standards. Interestingly, the resulting PDMAA, PD*n*PAA, and PMMEAA had broad MWDs of 1.22, 1.23, and 1.28, respectively, while PAPI, PNAM, PBMEAA, PDVAA, and PMPAA had narrow ones of 1.11, 1.15, 1.14, 1.09, and 1.10, respectively. The M_w/M_n value significantly depended on the used monomer. This dependence should be significantly assigned to the k_i/k_p difference in the polymerizations of the above monomers, *i.e.*, the polymerizations of API, NAM, BMEAA, DVAA, and MPAA seem to have good balance between k_i and k_p, while those of DMAA, D*n*PAA, and MMEAA have a poorer balance. It is rather understandable that both k_i and k_p vary when the used monomer is changed, which results in the k_i/k_p variation. Since it is seemingly impossible to accurately measure the k_is due to the induction period, we did not obtain the detailed k_i/k_p values and do not undertake a further discussion in this regard. The chemical structures of the obtained polymers were also confirmed by ^{1}H NMR and MALDI-TOF MS measurements like that for PDEAA, as shown in Figures S2 and S3.

Apart from DEAA, the polymerization kinetics of DMAA, API, BMEAA, and DVAA were also carried out in CH_2Cl_2 at room temperature and an argon atmosphere for the same $[M]_0/[^{Et}SKA]_0/[B(C_6F_5)_3]_0$ ratio of 25/1/0.05 and $[M]_0$ = 0.50 mol L^{-1}. The zero-order kinetic plots are shown in Figure 5 and all the t_is and $k_{p.obs.}$s are summarized in Table 3. It is very clear that all the propagation reactions of the polymerizations

Table 2. $B(C_6F_5)_3$-catalyzed GTP of DAA using ^{Et}SKA in CH_2Cl_2 at room temperature (~ 25 °C) [a]

run	Monomer (M)	$[M]_0/[^{Et}SKA]_0/[B(C_6F_5)_3]_0$	$[M]_0$ (mol L^{-1})	Time (h)	$M_{n,SEC}$ [c] ($M_{n,calcd.}$ [d]) (kg mol^{-1})	M_w/M_n [c]
17	DMAA	100/1/0.05	0.5	22	6.35 (10.0)	1.22
18	D*n*PAA	100/1/0.1	0.5	25	14.7 (15.6)	1.23
19	API	100/1/0.1	1.0	20	8.65 (14.0)	1.11
20	NAM	100/1/0.5	2.0	30	13.5 (14.2)	1.15
21	MMEAA	50/1/0.1	1.0	5	8.40 (7.26)	1.28
22	BMEAA	100/1/0.3	1.0	71	16.2 (18.8)	1.14
23	DVAA	100/1/0.1	0.5	19	13.5 (15.2)	1.09
24	MPAA	50/1/0.05	0.5	20	8.44 (6.26)	1.10

[a] Ar atmosphere; Conv. (determined by ^{1}H NMR in $CDCl_3$), >99 %. [b] Determined by SEC in DMF containing 0.01 mol L^{-1} of LiCl calibrated with PMMA. [c] Calculated from $[M]_0/[^{Et}SKA]_0$ × (MW of monomer: DMAA = 99.17, D*n*PAA = 155.24, API = 139.20, NAM = 141.17, MMEAA = 143.18, BMEAA = 187.24, DVAA = 151.21, and MPAA = 123.15) × Conv. + (MW of initiator residue: ^{Et}SKA = 102.13)

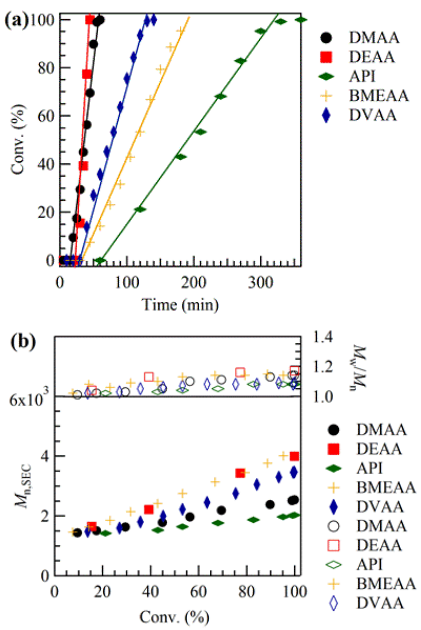

Figure 5. (a) Zero-order kinetic plots of the $B(C_6F_5)_3$-catalyzed GTPs of DMAA, DEAA, API, BMEAA, and DVAA at 25 °C and (b) $M_{n,SEC}$ and M_w/M_n dependence of the obtained PDAA on monomer conversion (Conv.). ($[M]_0/[^{Et}SKA]_0/[B(C_6F_5)_3]_0$ = 25/1/0.05

of DMAA, DEAA, API, BMEAA, and DVAA are zero-order reactions, except for the late propagation period. Under the same $[M]_0/[^{Et}SKA]_0$ ratio of 25, the t_is were estimated to be 16.9, 26.2, 65.9, 27.3, and 25.4 min, and the $k_{p.obs.}$s were 0.0256, 0.0523, 0.0040, 0.0069, and 0.0099 min^{-1} for DMAA, DEAA, API, BMEAA, and DVAA, respectively. According to $k_{p.obs.} = \frac{k_p[^{Et}SKA]_0[B(C_6F_5)_3]_0}{[DAA]_0}$, the k_ps for DMAA, DEAA, API, BMEAA, and DVAA were calculated to be 640, 1308, 100, 173, 248 L mol^{-1} min^{-1}, respectively. API had the longest induction period, DEAA, BMEAA, and DVAA in the middle, and DMAA the shortest, which well corresponded to the bulkiness order of their substituents at the nitrogen atom. On the other hand, the propagation rates were in the monomer order of DEAA > DMAA > DVAA > BMEAA > API, indicating that the hindrance of the functional and bulky substituents of the *N*-allyl, *N*-2-methoxyethyl, and *N*-piperidyl groups significantly decreased the propagation rate.

Table 3. A summary of the induction time (t_i), $k_{p.obs.}$s, and k_ps of the $B(C_6F_5)_3$-catalyzed GTPs of DMAA, DEAA, API, BMEAA, and DVAA [a]

Monomer (M)	$[M]_0/[^{Et}SKA]_0$	t_i (min)	$k_{p.obs.}$ (min^{-1})	k_p (L mol^{-1} min^{-1})
DMAA	25	16.9	0.0256	640
DEAA	25	26.2	0.0523	1308
API	25	65.9	0.0040	100
BMEAA	25	27.3	0.0069	173
DVAA	25	25.4	0.0099	248

[a] $[M]_0$, 0.50 mol L^{-1}; $[M]_0/[B(C_6F_5)_3]_0/[^{Et}SKA]_0$, 25/1/0.05; Ar atmosphere; room temperature (~ 25 °C); solvent, CH_2Cl_2.

Table 4. Synthesis of acrylamide block copolymers by sequential $B(C_6F_5)_3$-catalyzed GTP using ^{Et}SKA [a]

run	Monomer (M)		$[M]_0/[^{Et}SKA]_0$	Time (h)	$M_{n,SEC}$ [b] ($M_{n,calcd.}$ [c]) (kg mol^{-1})	M_w/M_n [b]
25	1st	DEAA	25	1.25	3.83 (3.28)	1.18
	2nd	DMAA	50	1	5.69 (8.24)	1.28
26	1st	DMAA	25	1	2.33 (2.58)	1.13
	2nd	DEAA	50	2	6.64 (8.94)	1.26
27	1st	DEAA	25	1.25	3.59 (3.28)	1.16
	2nd	DVAA	50	6	8.69 (11.04)	1.17
28	1st	DVAA	25	3	3.24 (3.98)	1.08
	2nd	DEAA	50	2	7.67 (8.24)	1.15

[a] Ar atmosphere; $[M]_0$, 0.5 mol L^{-1}; $[B(C_6F_5)_3]_0/[^{Et}SKA]_0$, 0.05; temp., r.t.; Conv. (determined by ^{1}H NMR in $CDCl_3$), >99%. [b] Determined by SEC in DMF containing 0.01 mol L^{-1} of LiCl calibrated with PMMA. [c] Calculated from $[M]_0/[^{Et}SKA]_0$ × (MW of monomer: DMAA = 99.17, DEAA = 127.18, DVAA = 151.21) × Conv. + (MW of initiator or propagation residue).

Synthesis of acrylamide homo diblock copolymer by the $B(C_6F_5)_3$-catalyzed GTP. The living nature of the $B(C_6F_5)_3$-catalyzed GTP of DAA was also used to prepare acrylamide diblock copolymers. DMAA and DVAA were used for the block copolymerization with DEAA by a sequential monomer addition method. The polymerization results are shown in Table 4. Twenty-five equivalents of the first monomer were quantitatively polymerized to produce the first-stage polymer product, after which 50 equivalents of the second monomer were added to continue the polymerization, leading to producing the acrylamide diblock copolymers. For all the polymerizations, the monomers were fully consumed in the fixed time no matter during which polymerization stage. The polymerizations of DEAA with DMAA and DVAA produced the corresponding diblock copolymers of PDEAA-*b*-PDMAA and PDEAA-*b*-PDVAA, respectively. In addition, the same diblock copolymers could also be obtained by changing the addition order of the acrylamide monomers. The resulting PDEAA-*b*-PDMAAs had relatively broad MWDs, while the PDEAA-*b*-PDVAAs had MWDs narrower than 1.17. As already mentioned, PDEAA, PDMAA, and PDVAA are thermoresponsive, water-soluble, and reactive acrylamide polymers. Therefore, these diblock copolymers are expected to have unique properties.

Synthesis of hetero diblock copolymer by the Lewis acid-catalyzed GTP. Given the fact that a SKA initiator has been applicable for the Lewis acid-catalyzed GTPs of both methacrylate and acrylamide monomers, we then attempted the synthesis of hetero-block copolymers composed of methacrylate and acrylamide blocks by the sequential GTP method. Twenty-five equivalents of methyl methacrylate (MMA) were first completely polymerized; afterwards, 50 equivalents of a DAA monomer (DEAA, DVAA, or NAM) were added to continue the second-stage polymerization. The block copolymerization under the reverse addition of MMA and a DAA monomer did not work because the first polymerization of an acrylamide monomer produces a PDAA bearing a silyl ketene aminal (SKAm) as the living end, which has been known not to initiate the polymerization of a methacrylate monomer. The block copolymerization of MMA and DEAA (run 29, Table 5) was first undergone using $B(C_6F_5)_3$ as the catalyst. However, the second-stage polymerization of DEAA did not proceed at all though the first-stage polymerization of MMA was fairly successful, probably because the large amount of $B(C_6F_5)_3$ required by GTP of MMA stopped the polymerization of DEAA. To solve this problem, $C_6F_5CHTf_2$ and Me_3SiNTf_2 with a much higher acidity than $B(C_6F_5)_3$ were then used. The block copolymerizations (runs 30-35, Table 5) afforded quantitative monomer conversions for both the MMA and DAA monomers and perfect molecular weight control of the PMMAs were obtained in the first-stage polymerizations. The initiation efficiencies of the first-stage polymerizations of MMA estimated from the $M_{n,calcd.}/M_{n.SEC}$s were extremely close to 100%. However, the sequential polymerization of a DAA monomer afforded mixed polymer products as confirmed by the SEC measurements in Figure 6, of which one trace points to the hetero-block copolymer of PMMA-*b*-PDAA and the other to the unreacted PMMA.For example, the $C_6F_5CHTf_2$-catalyzed block copolymerization of MMA and DEAA using ^{Et}SKA (run 30) afforded the mixed polymer products of PMMA-*b*-PDEAA and PMMA. The $M_{n.SEC}$ of PMMA-*b*-PDEAA was 47.2 kg mol^{-1}, which was significantly higher than the $M_{n.calcd.}$ of 8.96 kg mol^{-1} calculated based on the premise that all the SKA ends of PMMA obtained in the first-stage polymerization initiated the second-stage polymerization of DEAA. The mixed polymer products were isolated to obtain the pure PMMA-*b*-PDEAA and PMMA by preparative SEC in order to estimate the initiation efficiency in the second-stage polymerization and confirm the chemical structure of the unreacted PMMA. Because of the perfect

Table 5. Synthesis of hetero-block copolymers by sequential acid-catalyzed GTP of MMA and DAA [a]

run	Monomer (M)		Initiator	Catalyst	$[M]_0/[SKA]_0$	$[B(C_6F_5)_3]_0/[^{Et}SKA]_0$	time (h)	$M_{n,SEC}$ [b] ($M_{n,calcd.}$ [c]) (kg mol^{-1})	M_w/M_n [b]
29	1st	MMA	^{Et}SKA	$B(C_6F_5)_3$	25	0.30	2	2.49 (2.50)	1.09
	2nd	DEAA			50		45	n.d. [d]	n.d. [d]
30	1st	MMA	^{Et}SKA	$C_6F_5CHTf_2$	25	0.02	2	2.57 (2.50)	1.10
	2nd	DEAA			50		12	47.2 (8.96)	1.27 [e]
31	1st	MMA	^{Me}SKA	$C_6F_5CHTf_2$	25	0.02	2	2.59 (2.50)	1.07
	2nd	DEAA			50		5	44.8 (8.96)	1.26 [e]
32	1st	MMA	^{Et}SKA	Me_3SiNTf_2	25	0.02	1.5	2.16 (2.50)	1.07
	2nd	DEAA			50		7.5	78.4 (8.96)	1.30 [e]
33	1st	MMA	^{Me}SKA	Me_3SiNTf_2	25	0.02	1.5	2.51 (2.50)	1.06
	2nd	DEAA			50		3	43.5 (8.96)	1.30 [e]
34	1st	MMA	^{Me}SKA	Me_3SiNTf_2	25	0.02	1.25	2.43 (2.50)	1.07
	2nd	DVAA			50		13	17.0 (10.2)	1.26 [e]
35	1st	MMA	^{Me}SKA	Me_3SiNTf_2	25	0.02	1	2.34 (2.50)	1.06
	2nd	NAM			50		21	11.4 (9.66)	1.11

[a] Ar atmosphere; temp., r.t.; $[monomer]_0$ = 1.0 mol L^{-1}; Conv., >99% as determined by ^{1}H NMR in $CDCl_3$. [b] Determined by SEC in DMF containing 0.01 mol L^{-1} of LiCl calibrated with PMMA. [c] Calculated from $[monomer]_0/[initiator]_0$ × (MW of monomer: MMA = 100.12, DEAA = 127.18, DVAA = 151.21, NAM = 141.17) × Conv. + (MW of initiator or propagation residue). [d] Not determined due to no second-stage polymerization. [e] The shape of SEC was bimodal.

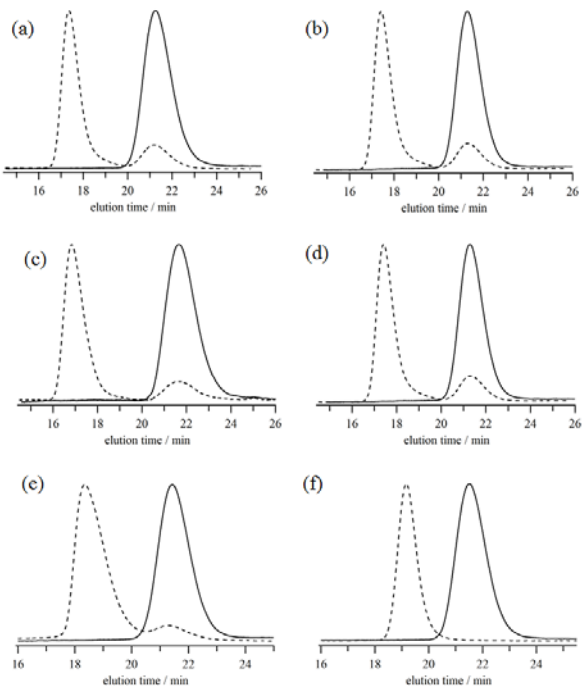

Figure 6. SEC traces of the obtained block copolymers, (a) run 30, (b) run 31, (c) run 32, (d) run 33, (e) run 34, (f) run 35 (eluent, DMF containing 0.01 mol L^{-1} LiCl; flow rate, 0.6 mL min^{-1}).

polymerization control in the first-stage and the nearly 100% initiation efficiency of the polymerization of MMA, it is rational to assume that the average degree of polymerization (DP) of the PMMA block is the same with the $[MMA]_0/[^{Et}SKA]_0$ ratio of 25. Based on this assumption, the ^{1}H NMR measurements of PMMA-*b*-PDEAA indicated that the PDEAA block had an average DP of 161. Thus, the initiation efficiency of the second-stage polymerization was estimated by $([DEAA]_0/[^{Et}SKA]_0)/DP$ as 31%. On the other hand, the analysis of the chemical structure of the unreacted PMMA by MALDI-TOF MS in Figure S4 indicated that this unreacted PMMA product was due to the desilylated PMMA obtained after quenching with MeOH. This result strongly suggested that no side reactions occurred during the entire polymerization course of MMA, and supported the fact that a part of the living SKA ends of PMMA did not initiate the second-stage polymerization of DEAA, leading to the eventual low initiation efficiency. This phenomenon can be well explained by the fact that the polymerization rate of DEAA from a SKAm end is significantly greater than the initiation rate, *i.e.*, the reaction rate of the Mukaiyama-Micheal reaction of the SKA end of PMMA with DEAA*.[38] This leads to the fact that the polymerization of DEAA was completed upon the initial SKAm formation from the Mukaiyama-Micheal reaction of only a part of the SKA ends of PMMA with DEAA*, and that the unreacted living PMMAs were left in the polymer products, as depicted in Scheme 3. The slower

 This journal is © The Royal Society of Chemistry 2012

Scheme 3. A schematic diagram for the diblock GTP of MMA and DAA.

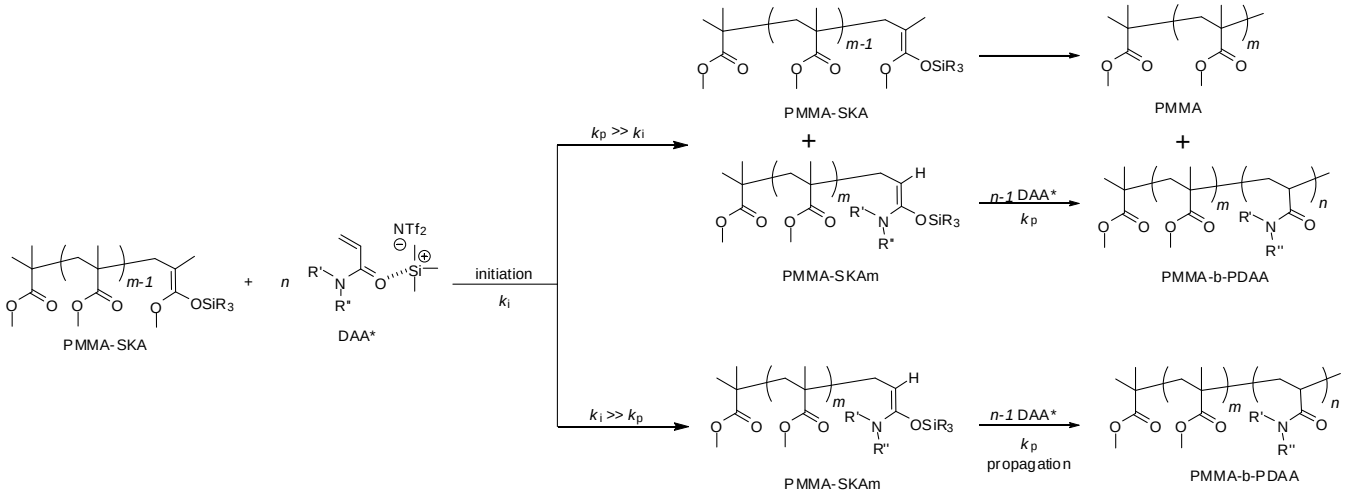

initiation rate than the polymerization rate is also the reason why the resulting block copolymers showed relatively broad polydispersities. In contrast, the $C_6F_5CHTf_2$-catalyzed block copolymerization of MMA and DEAA using the more reactive ^{Me}SKA (run 31) showed an improved initiation efficiency of the second-stage polymerization of DEAA (36%) and produced a PMMA-*b*-PDEAA with a $M_{n.SEC}$ (44.8 kg mol^{-1}) lower than that of PMMA-*b*-PDEAA obtained in run 30 due to the enhanced initiation rate between ^{Me}SKA and DEAA*. These polymerization behaviors were also observed for the Me_3SiNTf_2-catalyzed block copolymerizations of MMA and DEAA using ^{Et}SKA and ^{Me}SKA (runs 32-33).

It is rather clear that in order to obtain a higher initiation efficiency and better polymerization control of the second-stage polymerization is to have the appropriate balance between the initiation (from SKA end of PMMA) and polymerization rates. Considering this, the block copolymerizations using the more reactive ^{Me}SKA and less reactive DAA monomers of DVAA or NAM were further investigated by the Me_3SiNTf_2-catalyzed GTP, as shown in runs 34-35. ^{Me}SKA was used to enhance the initiation rate, while DVAA and NAM were used to reduce the polymerization rate. Obviously, the polymerization control over the molecular weight and polydispersity of the final block copolymers was remarkably improved in these two block copolymerizations as the $M_{n.SEC}$s of 17.0 (PMMA-*b*-PDVAA, run 34) and 11.4 (PMMA-*b*-PNAM, run 35) kg mol^{-1} were much closer to their corresponding $M_{n.calcd.}$s of 10.2 and 9.66 kg mol^{-1}, respectively. Especially when NAM was used as the second monomer, the block copolymerization turned out to be almost perfect (Figure 6(f)). In short summary, these results strongly suggest that the perfect block copolymerization of different acrylic monomers can be achieved by carefully selecting the reactivity-matched comonomers. This has been the first finding in this regard in the GTP field.

Conclusions

Various combinations of acidic organocatalysts (Me_3SiNTf_2, $C_6F_5CHTf_2$, and $B(C_6F_5)_3$) and SKAs (^{Me}SKA, ^{Et}SKA, ^{iPr}SKA, and ^{Ph}SKA) were proven to be significantly efficient for the GTPs of DEAA to produce well-defined PDEAAs, among which the polymerization using $B(C_6F_5)_3$ and ^{Et}SKA showed a relatively better control over the molecular weight distribution. The $B(C_6F_5)_3$-catalyzed GTP using ^{Et}SKA was applicable to various *N*,*N*-disubstituted acrylamides (DAAs) including the water-soluble, thermoresponsive, and reactive ones. All the $B(C_6F_5)_3$-catalyzed polymerizations showed an obvious induction period of tens of minutes, after which it proceeded as a zero-order reaction in a living fashion. The occurrence of the induction period was clearly attributed to the structural mismatch between the SKA and DAA. In addition, the initiation and propagation rates of a DAA were significantly dependent on its *N*-disubstituents and the balance between them was the key factor for well controlling the polymerization, *i.e.*, the GTPs of API, NAM, BMEAA, and DVAA with relatively bulky substituents were well-controlled due to the good balance of the initiation and propagation rates, while those of DMAA, DEAA, D*n*PAA, and MMEAA with less bulky substituents had worse polymerization control. Acrylamide polymers with an average DP of no more than 200 could be synthesized by the $B(C_6F_5)_3$-catalyzed GTP method. The livingness of the polymerization system was suitable for synthesizing homo block copolymers composed of different acrylamide blocks and hetero block copolymers of PMMA-*b*-PDAA by the sequential GTP method. Importantly, it has been shown for the first time that a perfect hetero-block copolymer of PMMA-*b*-PNAM could be synthesized by selecting the reactivity-matched comonomers of MMA and NAM using the combination of the much stronger Lewis acid catalyst, Me_3SiNTf_2, and ^{Me}SKA. This information is crucially helpful for designing the well-defined hetero-block copolymers, which are currently under investigation. As an expectation, these resulting homo acrylamide polymers, homo block

acrylamide copolymers, and hetero block copolymers in this study are applicable for various purposes such as polymer electrolytes, smart polymer materials, and flocculating agents. This study has provided significant progress in the organocatalyzed GTP of DAAs and is expected to help polymer chemists in designing new acrylamide polymers.

Acknowledgements

This work was financially supported by the MEXT (Japan) program "Strategic Molecular and Materials Chemistry through Innovative Coupling Reactions" of Hokkaido University and the MEXT Grant-in-Aid for Scientific Research on Innovative Areas "Advanced Molecular Transformation by Organocatalysts". S.K., and K.T. gratefully acknowledge the JSPS Fellowship for Young Scientists.

Notes and references

[a] *Graduate School of Chemical Sciences and Engineering, Hokkaido University, N13W8, Kita-ku, Sapporo 060-8628, Japan.*
[b] *Frontier Chemistry Center, Faculty of Engineering, Hokkaido University, Sapporo, 060-8628, Japan..*
[c] *Division of Applied Chemistry, Faculty of Engineering, Hokkaido University, N13W8, Kita-ku, Sapporo 060-8628, Japan.*
E-mail: kakuchi@poly-bm.eng.hokudai.ac.jp

†Electronic Supplementary Information (ESI) available: Synthetic procedures of DAA monomers, and SEC, ^{1}H NMR, and MALDI-TOF MS results of the obtained PDAAs. are available. See DOI: 10.1039/b000000x/

1 Qian, J. W.; Xiang, X. J.; Yang, W. Y.; Wang, M.; Zheng, B. Q. *Eur. Polym. J.* 2004, **40**, 1699-1704.
2 Christensen, L. H. *Dermatologic Surgery* 2009, **35**, 1612-1619.
3 Huang, X.; Wirth, M. J. *Macromolecules* 1999, **32**, 1694-1696.
4 Teodorescu, M.; Matyjaszewski, K. *Macromol. Rapid Commun.* 2000, **21**, 190-194.
5 Benoit, D.; Chaplinski, V.; Braslau, R.; Hawker, C. J. *J. Am. Chem. Soc.* 1999, **121**, 3904-3920.
6 Convertine, A. J.; Lokitz, B. S.; Lowe, A. B.; Scales, C. W.; Myrick, L. J.; McCormick, C. L. *Macromol. Rapid Commun.* 2005, **26**, 791-795.
7 Cao, Y.; Zhu, X. X.; Luo, J.; Liu, H. *Macromolecules* 2007, **40**, 6481-6488.
8 Thomas, D. B.; Sumerlin, B. S.; Lowe, A. B.; McCormick, C. L. *Macromolecules* 2003, **36**, 1436-1439.
9 Xie, X.; Hogen-Esch, T. E. *Macromolecules* 1996, **29**, 1746-1752.
10 Kobayashi, M.; Ishizone, T.; Nakahama, S. *Macromolecules* 2000, **33**, 4411-4416.
11 Kobayashi, M.; Okuyama, S.; Ishizone, T.; Nakahama, S. *Macromolecules* 1999, **32**, 6466-6477.
12 Kobayashi, M.; Ishizone, T.; Nakahama, S. *J. Polym. Sci., Part A: Polym. Chem.* 2000, **38**, 4677-4685.
13 Ishizone, T.; Yashiki, D.; Kobayashi, M.; Suzuki, T. Ito, M. Nakahama, S. *J. Polym. Sci., Part A: Polym. Chem.* 2007, **45**, 1260-1271.
14 Suzuki, T.; Kusakabe, J.; Ishizone, T. *Macromolecules* 2008, **41**, 1929-1936.
15 Suzuki, T.; Kusakabe, J.; Kitazawa, K.; Nakagawa, T.; Kawauchi, S.; Ishizone, T. *Macromolecules* 2010, **43**, 107-116.
16 Ito, M.; Ishizone, T. *J. Polym. Sci., Part A: Polym. Chem.* 2006, **44**, 4832-4845.
17 Kobayashi, M. Chiba, T.; Tsuda, K.; Takeishi, M. *J. Polym. Sci., Part A: Polym. Chem.* 2005, **43**, 2754-2764.
18 Webster, O. W.; Hertler, W. R.; Sogah, D. Y.; Farnham W. B.; RajanBabu, T. V. *J. Am. Chem. Soc.* 1983, **105**, 5706-5708.
19 Sogah, D. Y.; Hertler, W. R.; Webster, O. W.; Cohen, G. M. *Macromolecules* 1987, **20**, 1473-1488.
20 Webster, O. W. *J. Polym. Sci., Part A: Polym. Chem.* 2000, **38**, 2855-2860.
21 Webster, O. W. *Adv. Polym. Sci.* 2004, **167**, 1-34.
22 Zhuang, R.; Müller, A. H. E. *Macromolecules* 1995, **28**, 8035-8042.
23 Zhuang, R.; Müller, A. H. E. *Macromolecules* 1995, **28**, 8043-8050.
24 Fuchise, K.; Chen, Y.; Satoh, T.; Kakuchi, T. *Polym. Chem.* 2013, **4**, 4278-4291.
25 Ute, K.; Ohnuma, H.; Kitayama, T. *Polym. J.* 2000, **32**, 1060-1062.
26 Raynaud, J.; Ciolino, A.; Beceiredo, A.; Destarac, M.; Bonnette, F.; Kato, T.; Gnanou, Y.; Taton, D. *Angew. Chem. Int. Ed.* 2008, **47**, 5390-5393.
27 Scholten, M. D.; Hedrick, J. L.; Waymouth, R. M. *Macromolecules* 2008, **41**, 7399-7404.
28 Raynaud, J.; Liu, N.; Gnanou, Y.; Taton, D. *Macromolecules* 2009, **42**, 5996-6005.
29 Zhang, Y.; Chen, E. Y.-X. *Macromolecules* 2008, **41**, 36-42.
30 Zhang, Y.; Chen, E. Y.-X. *Macromolecules* 2008, **41**, 6353-6360.
31 Fevre, M.; Vignolle, J.; Heroguez, V.; Taton, D. *Macromolecules* 2012, **45**, 7711-7718.
32 Kakuchi, R.; Chiba, K.; Fuchise K.; Sakai, R.; Satoh, T.; Kakuchi, T. *Macromolecules* 2009, **42**, 8747-8750.
33 Kakuchi, T.; Chen, Y.; Kitakado, J.; Mori, K.; Fuchise, K.; Satoh, T. *Macromolecules* 2011, **44**, 4641-4647.
34 Takada, K.; Fuchise, K.; Chen, Y.; Satoh, T.; Kakuchi, T. *J. Polym. Sci. Part A: Polym. Chem.* 2012, **50**, 3560-3566.
35 Eggert, M.; Freitag, R. *J. Polym. Sci., Part A: Polym. Chem.* 1994, **32**, 803-813.
36 Freitag, R.; Baltes, T.; Eggert, M. *J. Polym. Sci., Part A: Polym. Chem.* 1994, **32**, 3019-3030.
37 Baltes, T.; Garret-Flaudy, F.; Freitag, R. *J. Polym. Sci., Part A: Polym. Chem.* 1999, **37**, 2977-2989.
38 Fuchise, K.; Sakai, R.; Satoh, T.; Sato, S.; Narumi, A.; Kawaguchi, S.; Kakuchi, T. *Macromolecules* 2010, **43**, 5589-5594.
39 Fuchise, K.; Chen, Y.; Takada, K.; Satoh, T.; Kakuchi, T. *Macromol. Chem. Phys.* 2012, **213**, 1604-1611.
40 Raynaud, J.; Liu, N.; Gnanou, Y.; Taton, D. *Macromolecules* 2010, **43**, 8853-8861.
41 Raynaud, J.; Liu, N.; Fèvre, M.; Gnanou, Y.; Taton, D. *Polym. Chem.* 2011, **2**, 1706-1712.
42 Hasegawa, A.; Naganawa, Y.; Fushimi, M.; Ishihara, K.; Yamamoto, H. *Org. Lett.* 2006, **8**, 3175-3178.
43 Liu, S.-Y.; Hills, I. D.; Fu, G. *J. Am. Chem. Soc.* 2005, **127**, 15352-15353.

 This journal is © The Royal Society of Chemistry 2012

44 Parks, D. J.; Piers, W. E.; Parvez, M.; Atencio, R.; Zaworotko, M. J. *Organometallics* 1998, **17**, 1369-1377.

TOC use only

Organic Acids as Efficient Catalyst for Group Transfer Polymerization of *N,N*-Disubstituted Acrylamide with Silyl Ketene Acetal; Polymerization Mechanism and Synthesis of Diblock Copolymers

The GTP of *N,N*-disubstituted acrylamide using organic acid and silyl ketene acetal was intensively investigated.

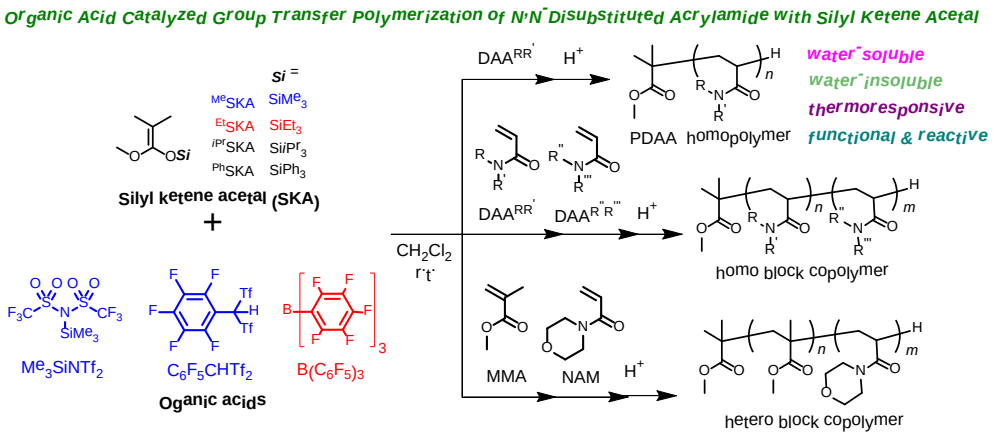

This journal is © The Royal Society of Chemistry 2012